Applied Catalysis B: Environmental 84 (2008) 433–439

Contents lists available at ScienceDirect

Applied Catalysis B: Environmental

journal homepage: www.elsevier.com/locate/apcatb

Co-production of hydrogen and multi-wall carbon nanotubes from ethanol decomposition over Fe/Al_2O_3 catalysts

Weilong Li [a,b], Hui Wang [a,*], Zhaoyu Ren [b], Gang Wang [a], Jinbo Bai [c]

[a] Chemistry Department, Shaanxi Key Laboratory of Physico-Inorganic Chemistry, Northwest University, Xi'an 710069, PR China
[b] Institute of Photonics & Photon-Technology, Northwest University, Xi'an 710069, PR China
[c] Lab. MSS/MAT, CNRS UMR 8579, Ecole Centrale Paris, 92295 Chatenay Malabry, France

ARTICLE INFO

Article history:
Received 30 July 2007
Received in revised form 6 April 2008
Accepted 27 April 2008
Available online 3 May 2008

Keywords:
Ethanol decomposition
Supported Fe catalyst
Hydrogen
Carbon nanotube

ABSTRACT

The co-production of hydrogen and carbon nanotubes (CNTs) from the decomposition of ethanol over Fe/Al_2O_3 at different temperatures and feeding rates of ethanol was investigated systematically. The results indicated that Fe/Al_2O_3 was a quite active catalyst for the co-production of hydrogen and CNTs and that its activity and stability depended strongly on the Fe loading. Among all catalysts tested, 10 mol% Fe/Al_2O_3 was the most effective catalyst based on the ratio of hydrogen production, the total H_2 yield, and the quality of the CNTs formed. The efficiency of hydrogen production from ethanol decomposition over 10 mol% Fe/Al_2O_3 reached a maximum of ~80% at 800 °C and the yield of CNTs with well-oriented growth and uniform diameter was 141%. In addition, the reaction of hydrogen and CNTs co-produced from ethanol decomposition was proposed.

1. Introduction

Energy sources and environment are basically two main problems we face today. Hydrogen is known as a clean energy carrier and will play an important role in the future's global economy, especially for power generation in fuel cells. Hydrogen is considered as an ideal fuel for hydrogen fuel cell due to its high utilization efficiency, zero emission and potentially abundant production from other renewable resources [1–4]. However, there is no large-scale utilization of hydrogen because of several main problems. One of them is how to produce hydrogen at low cost. At present, there are four traditional methods for hydrogen production: water electrolysis, gasification reactions, partial oxidation reactions of heavy oil, and hydrocarbon steam reforming reactions [5–8]. Recently, chemical decomposition [9,10] of fossil gas like methane is an attractive method to produce hydrogen (H_2), however, fossil gas is non-sustainable nature. Among the various fuels that can be converted into hydrogen, ethanol is a very promising candidate because of its low-toxicity, easy-generation from renewable resources, low production costs and relatively high hydrogen content. Many groups [11–15] did a lot of work on producing hydrogen (H_2) by steam reforming of ethanol and its mechanism, but none of them mentioned the production of carbon nanotubes (CNTs) accompanied by hydrogen during ethanol decomposition.

CNTs attracted intense attention of researchers worldwide since detailed observations in 1991 [16] due to their unique structure, special physical and chemical properties [17], and extensive applications such as composite materials, field emission devices, nanometer-sized electronic devices, sensors and the probe of electron microscope [18]. To realize these potential applications, large-scale synthesis of CNTs is one of the main problems. Many methods have been developed to synthesize CNTs, such as arc discharge [19], laser ablation [20] and chemical vapor deposition (CVD) [21,22]. Comparing with the other methods, CVD of hydrocarbon gases over catalysts is a common technique due to its potential scaling-up possibility. CVD synthesis of CNTs using ethanol as carbon source was first reported by Maruyama et al. [23]. They synthesized high-purity single wall CNTs, but H_2 production from ethanol decomposition was not investigated.

Although the decomposition of methane into hydrogen and CNTs has been widely reported [9,10], fewer studies have dealt with the production of hydrogen and CNTs from ethanol decomposition. Therefore, in the present work the co-production of H_2 and CNTs from ethanol decomposition over Al_2O_3-supported Fe catalysts was investigated systematically. The effect of the reaction conditions on the performance of Fe/Al_2O_3 catalysts in co-producing H_2 and CNTs by catalytic decomposition of ethanol was discussed in detail. The reactions about ethanol decomposition were proposed. The optimal growth conditions of CNTs were presented.

* Corresponding author. Tel.: +86 29 8836 3115; fax: +86 29 8830 3798.
E-mail address: huiwang@nwu.edu.cn (H. Wang).

0926-3373/$ – see front matter © 2008 Elsevier B.V. All rights reserved.
doi:10.1016/j.apcatb.2008.04.026

2. Experimental

2.1. Preparations of the catalysts

Fe catalysts supported on Al_2O_3 were prepared by the means of co-precipitation. $Fe(NO_3)_3{\cdot}9H_2O$ and $Al(NO_3)_3{\cdot}9H_2O$ were utilized as the precursors of iron catalyst and its support, respectively, and urea as the precipitator. Various loadings of catalysts were prepared, and the amount of Fe cations was adjusted to *x* mol% of total metal (Fe and Al) cations (10 mol% means Fe/(Fe + Al) = 10%). The catalysts were denoted as Fe (*x* mol%)/Al_2O_3.

The detailed procedure of the catalyst preparation is as follows: certain amounts of $Fe(NO_3)_3 \cdot 9H_2O$ and $Al(NO_3)_3 \cdot 9H_2O$ were mixed in 50 ml water. Some urea (30 times of Al cation-mol) was dissolved in 450 ml pure water, and the solution was heated to above 80 °C by water-bath (the urea would be hydrolyzed into NH_3 and CO_2). Then the solution of the metal salts was added dropwise into urea solution at a constant rate. The temperature of the urea solution was kept at 80 °C until a lot of precipitation was produced. The suspension with the precipitation was kept at a stable state for 24 h, the upper solution was swilled and the precipitation was washed with deionized water repeatedly in order to remove the urea completely. The precipitation was dried at 80 °C for 12 h and calcined in air at 500 °C for 10 h, and subsequently triturated into powder. The Fe/Al_2O_3 catalysts with various loadings were obtained and kept in a desiccator for further use.

2.2. Co-production of H_2 and CNTs

H_2 and CNTs were co-produced by ethanol decomposition over Fe/Al_2O_3 catalysts. For a typical batch, about 0.25 g of fresh Fe/Al_2O_3 catalysts were placed in constant-temperature zone of quartz tube inside of vertically fixed bed reactor. The catalysts were heated at 4 °C/min by program controller from room temperature to the reduction temperature (500 °C) in flowing Ar (40 ml/min), and then were reduced by H_2 for 1 h at the flow rate of 40 ml/min with 1:1 gas mixture of H_2 and Ar. After reduction, H_2 flow was turned off and Ar flow was turn up to 40 ml/min again, then the tube was heated from the reduction temperature to a desirable reaction temperature (5 °C/min). When the temperature was stable, ethanol was injected in gasification room by feeding-rate-controllable injector and then gaseous ethanol was led into reactor by carrier gas (Ar, 40 ml/min). Ethanol was decomposed over Fe/Al_2O_3 catalysts for 40 min. The components and contents of gases produced from the reaction were detected by gas chromatography (GC). After the reaction the reactor was cooled to room temperature in Ar stream.

2.3. Characterizations of CNTs

Raman spectra of carbons deposited on the catalysts through ethanol decomposition were recorded by Almega Dispersive Raman spectrometer (American Thermo Nicolet Company) and the excitation wavelength was 532 nm.

The SEM (scanning electron microscopy) images of carbons deposited on the catalysts from ethanol decomposition were obtained with a FEI Quanta 400 FEG–ESEM (field emission gun–environmental scanning electron microscope).

The TEM (transmission electron microscopy) images of as-grown CNTs without any purification and pretreatment were carried out with a JEOL JEM-3010 electron microscope at 300 kV. The samples were stirred by ultrasonic about 10 min in ethanol, and then, the copper grids were dipped in the suspension and evaporated underneath the infrared light before observation.

TG–DTG (thermogravimetry and differential thermogravimetry) analysis data were collected in a NETZSCH STA 449C instrument. The samples were heated from room temperature to 1100 °C in air, and the heating rate was 10 °C/min. The weight change as temperature function was recorded and the yield of CNTs could be calculated from it.

3. Results and discussion

3.1. H_2 obtained from ethanol decomposition

H_2 accompanied by CNT production were obtained from ethanol decomposition over Fe/Al_2O_3 catalysts with different loadings of Fe. The amount of H_2 produced was detected by GC and evaluated by *the ratio of hydrogen production* and expressed as follows:

$$\text{The ratio of hydrogen production}\ (\%) = \frac{\text{Mol}_1}{\text{Mol}_2} \times 100$$

where Mol_1 is the moles of H_2 produced during the course of ethanol decomposition, Mol_2 is the theoretical moles of H_2 contained in ethanol feedstock.

3.1.1. Effect of Fe catalyst on hydrogen production

Fig. 1 shows the curves of the ratio of hydrogen production as a function of reaction temperature in ethanol decomposition over Fe/Al_2O_3 catalysts with different loadings of Fe and pure Al_2O_3 (in the absence of Fe). The reaction was performed in the temperature range from 100 to 750 °C at a linearly programmed rate of 5 °C/min. From the curves, it can be found that no hydrogen production was observed at <550 °C for pure Al_2O_3 without Fe loading, and the ratio of hydrogen production for pure Al_2O_3 was also not more than 20% even if the temperature reached 750 °C. However, when Fe was loaded on, Fe/Al_2O_3 catalysts had obviously catalytic activity for ethanol decomposition and the ratio of hydrogen production was improved rapidly with increasing Fe loadings of catalysts. For instance, when the ratio of hydrogen production was 20%, the reaction temperatures for pure Al_2O_3, 10 and 30 mol% loadings of Fe/Al_2O_3 catalysts were 750, 470 and 350 °C, respectively. Therefore, the reaction temperature decreased significantly due to the presence of Fe catalysts.

As shown in Fig. 1, the kinetics curves for catalysts with different loadings of Fe presented the wave-like change. For Fe (10 mol%)/Al_2O_3, when the reaction temperature was 600 °C, the ratio of hydrogen production was about 35%, and then the ratio decreased slightly (about 30%) as temperature rising further to 700 °C, subsequently, climbed to 35% again when the temperature arrived at 750 °C. Similar observations could be found for 30 and

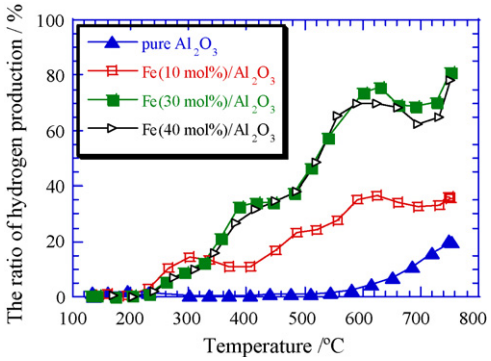

Fig. 1. Change of the ratio of hydrogen production as a function of reaction temperature in ethanol decomposition over Fe/Al_2O_3 catalysts with different loadings of Fe. The feeding rate of ethanol: 0.3 ml/h, carrier gas (Ar): 40 ml/min.

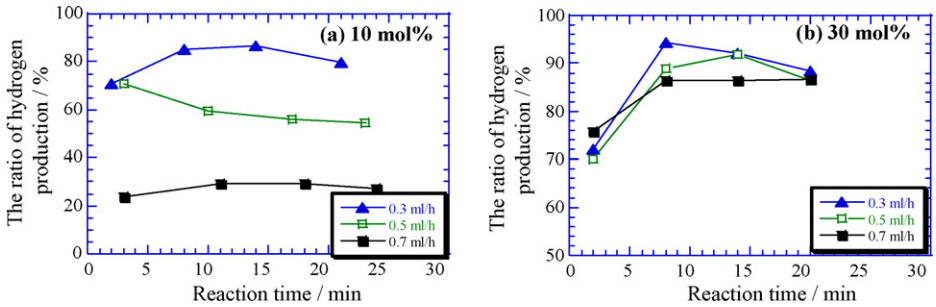

Fig. 2. Change of the ratio of hydrogen production as a function of reaction time at different feeding rates (0.3, 0.5, 0.7 ml/h) in ethanol decomposition over Fe/Al_2O_3 catalysts (at 750 °C): Fe loadings (a) 10 mol% and (b) 30 mol%.

40 mol% loadings of catalysts. In addition, from Fig. 1, it can be also found that the kinetics curves for Fe (30 mol%)/Al_2O_3 and Fe (40 mol%)/Al_2O_3 catalysts overlap nearly, showing that the increase of Fe loading almost has no incremental effect on the ratio of hydrogen production when Fe loadings of catalysts exceed 30 mol%.

3.1.2. Effect of the feeding rate of ethanol on the hydrogen production

Fig. 2 shows the ratio of hydrogen production as a function of reaction time in ethanol decomposition over Fe/Al_2O_3 catalysts with different feeding rates of ethanol (0.3, 0.5, 0.7 ml/h) at 750 °C. Fig. 2(a and b) corresponds to the catalysts with Fe loadings of 10 and 30 mol%, respectively. For both Fe/Al_2O_3 catalysts with Fe loadings of 10 and 30 mol%, comparison of the ratios of hydrogen production with respect to different feeding rates of ethanol indicated that the ratio of hydrogen production depended on ethanol feed, and varied in the following order of the feeding rate: 0.3 ml/h > 0.5 ml/h > 0.7 ml/h. When the feeding rate of ethanol was higher, more ethanol was introduced into the reaction system in a short time. Part of the ethanol was not decomposed over the catalysts in time and brought out by the carrier gas from the system. Also, the feeding rate of ethanol had smaller influence on the ratio of hydrogen production for Fe (30 mol%)/Al_2O_3 than that for Fe (10 mol%)/Al_2O_3. The reason may be that higher loadings of Fe provide larger surface for ethanol decomposition, so the effect of the feeding rate of ethanol on hydrogen production is decreased. The feeding rate of ethanol was fixed on 0.3 ml/h in the following text.

3.1.3. Effect of temperature and Fe loading on hydrogen production

Fig. 3 shows the variations of the ratio of hydrogen production as a function of reaction time in ethanol decomposition over the Fe/Al_2O_3 catalysts with different loadings of Fe at different temperatures. It can be seen from Fig. 3(a) that the ratio of hydrogen production generally became higher with increasing Fe loading at 500 °C. The features of the curves of ethanol decomposition for 600–800 °C in Fig. 3(b–d) were similar to those for 500 °C. However, the increased amount of the ratio of hydrogen production was declined at higher temperatures (800 °C). For instance, at 500 °C the average ratio of hydrogen production for Fe (10 mol%)/Al_2O_3 was about 20% and that for Fe (40 mol%)/Al_2O_3 was about 70%, the ratio of hydrogen production had an increase of 50% with increasing Fe loading. However, at 800 °C the increase of

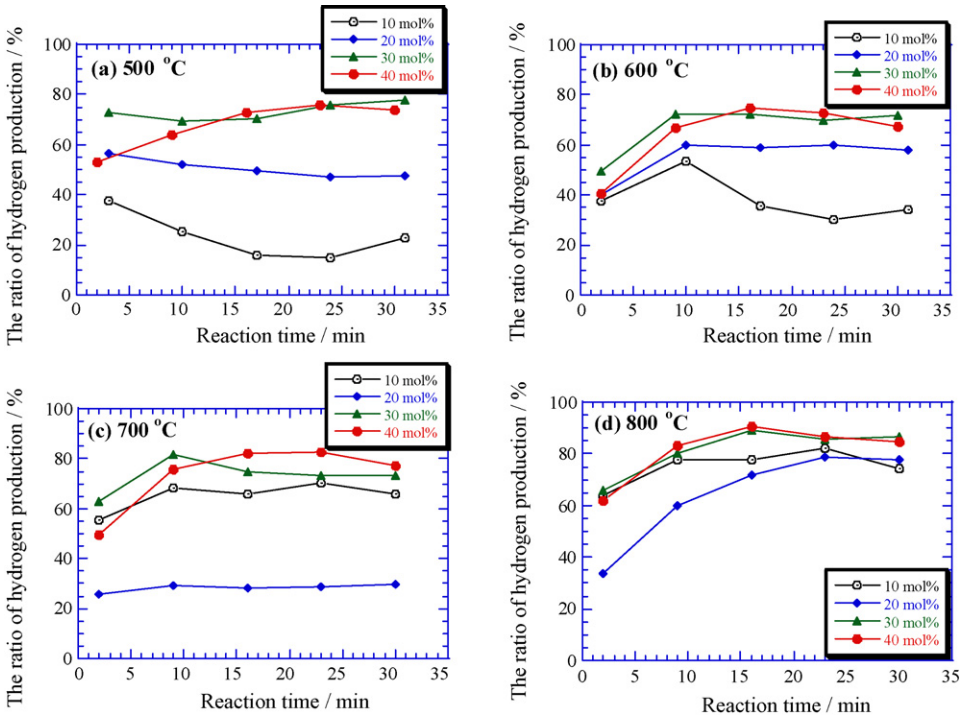

Fig. 3. Change of the ratio of hydrogen production as a function of reaction time in ethanol decomposition over Fe/Al_2O_3 catalysts with different Fe loadings at different temperatures: (a) 500 °C, (b) 600 °C, (c) 700 °C, (d) 800 °C.

Table 1
The average ratio of hydrogen production at different temperatures and loadings of catalysts

Loadings of catalysts (mol%)	The average ratio of hydrogen production (%)			
	500 °C	600 °C	700 °C	800 °C
10	23.2	38.4	65.2	80.1
20	50.6	55.4	28.3	64.4
30	73.3	67.0	73.5	81.5
40	67.9	64.5	73.2	81.4

the ratio of hydrogen production was less than 10% with Fe loading increasing from 10 to 40 mol%.

It can be also found from Fig. 3 that catalysts with 20 mol% loading presented the strange result: the ratios of hydrogen production at lower temperatures (500 and 600 °C) were higher than those at higher temperatures (700 and 800 °C), which was different from that of the catalysts with other loadings. The cause for it will be investigated further in our future work.

Table 1 shows the average ratios of hydrogen production for Fe/Al_2O_3 catalysts with different loadings of Fe at different temperatures. It is apparent that the ratio of hydrogen production for the Fe (10 mol%)/Al_2O_3 and Fe (20 mol%)/Al_2O_3 catalysts in most cases became higher with increasing temperature (except for the 20 mol% Fe loading at 700 °C), but it changed slightly with temperature for the Fe (30 mol%)/Al_2O_3 and Fe (40 mol%)/Al_2O_3 catalysts and even became smaller from 500 to 600 °C. The ratio of hydrogen production over Fe (40 mol%)/Al_2O_3 was smaller than over Fe (30 mol%)/Al_2O_3 at 500 and 600 °C and it was almost same at 700 and 800 °C. As a result, the order of average ratio of hydrogen production for the catalysts at 500 and 600 °C was 30 mol% > 40 mol% >20 mol% > 10 mol%, and the order at 700 and 800 °C was 30 mol% ≈ 40 mol% > 10 mol% > 20 mol%. The average ratio of hydrogen production reached and even exceeded 80% for the Fe (10, 30 and 40 mol%)/Al_2O_3 catalysts at 800 °C.

Table 2 shows the total yield of H_2 in initial 30 min over Fe/Al_2O_3 catalysts with different Fe loadings at different temperatures. The total yield of H_2 means the molar of H_2 produced from per molar iron contained in catalyst. It is found that the total yield of H_2 became higher with increasing temperatures (except for 20 mol% loading), and temperature had more obvious impact on total yield of H_2 for catalyst with lower Fe loading than that for catalyst with higher Fe loading. For example, the total H_2 yield had an increase of 8.1×10^6 μmol Fe-mol^{-1} for Fe (10 mol%)/Al_2O_3 when the temperature increased from 500 to 800 °C, while the total H_2 yield for Fe (40 mol%)/Al_2O_3 had just an increase of 0.6×10^6 μmol Fe-mol^{-1} in the same case. The total H_2 yield for Fe (10 mol%)/Al_2O_3 at 800 °C was maximal, about 11.2×10^6 μmol Fe-mol^{-1}. The reason for it may be that, for catalysts with lower Fe loading, Fe particles loaded on the support (Al_2O_3) are well dispersed, which led to higher activity of the catalysts. When Fe loading exceeds certain value (30 mol%), Fe particles loaded on the support (Al_2O_3) may be saturated, increasing Fe loading has little effect on enhancing activity of the catalysts obviously and, in some case, even led to reducing activity of the catalysts due to becoming bigger Fe catalyst particles. The increase in the size of Fe particles may be because of agglomeration or sintering of the catalyst particles at higher Fe loading or higher temperature.

Table 2
Total yield of H_2 per molar iron during 30 min in ethanol decomposition over Fe/Al_2O_3 catalysts with different Fe loadings at different temperatures

Loadings of catalysts (mol%)	Total yield of H_2 ($\times 10^6$ μmol·Fe-mol^{-1})			
	500 °C	600 °C	700 °C	800 °C
10	3.1	5.9	9.7	11.2
20	3.6	4.2	2.2	5.1
30	3.9	3.7	4.0	4.5
40	2.9	2.8	3.2	3.5

3.1.4. *Effect of Fe loading on catalytic activity and stability during the hydrogen production from ethanol decomposition*

Fig. 4 shows the changes of the rate of hydrogen production as reaction time in ethanol decomposition over different loadings of catalysts (ethanol was introduced to the reactor and the gases produced from ethanol decomposition was detected by GC at the beginning of heating. When the temperature arrived at 750 °C, keep this temperature 3 h). It is observed that the highest rate of hydrogen production for Fe (10 mol%)/Al_2O_3 was about 3300 μmol min^{-1} Fe-g^{-1} at 150 min, and then the rate of hydrogen production decreased moderately with the reaction time because of catalyst deactivation. The highest rate of hydrogen production for Fe (30 mol%)/Al_2O_3 was about 2700 μmol min^{-1} Fe-g^{-1} at 150 min, and then stayed at this value during 3 h without observing catalyst deactivation. The highest rate of hydrogen production for Fe (40 mol%)/Al_2O_3 was about 2200 μmol min^{-1} Fe-g^{-1} at 170 min, and then the rate of hydrogen production decreased sharply with the reaction time due to the quick catalyst deactivation. The catalytic stability of Fe/Al_2O_3 catalysts for different Fe loadings varied in the following order: 30 mol% > 10 mol% > 40 mol%, while the order of catalytic activity of Fe/Al_2O_3 catalysts was 10 mol% > 30 mol% > 40 mol%.

As described above, we discussed systematically the influences of various reaction conditions (such as the loading amount of Fe, the feeding rate of ethanol and temperature) on the hydrogen production in ethanol decomposition over Fe/Al_2O_3 catalysts. Some results can be summarized as follows: (1) Fe/Al_2O_3 catalysts have obviously catalytic effect for H_2 production from ethanol decomposition. (2) Smaller feeding rate of ethanol gave higher ratios of hydrogen production. (3) The ratio of hydrogen production in most cases became higher with increasing temperature for the same loading of Fe and compared to other Fe loadings, there was the highest ratio of hydrogen production for the catalysts with 30 mol% Fe loading at various temperatures. The average ratio of hydrogen production reached and even exceeded 80% for the Fe (10, 30 and 40 mol%)/Al_2O_3 catalysts at 800 °C. (4) The total H_2 yield during the first 30 min for Fe (10 mol%)/Al_2O_3 at 800 °C was maximal, about 1.1×10^7 μmol Fe-mol^{-1}. (5) The orders of catalytic stability and activity for Fe/Al_2O_3 catalysts with different Fe loadings were 30 mol% > 10 mol% > 40 mol% and 10 mol% > 30 mol% > 40 mol%, respectively. In terms of the ratio of hydrogen production, the total yield H_2 and catalytic stability and activity, the Fe (10 mol%)/Al_2O_3 catalyst was the best one for H_2 production from ethanol decomposition.

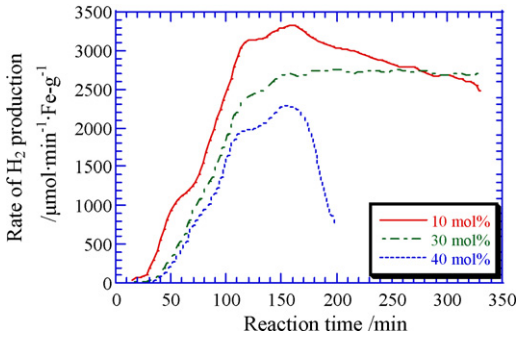

Fig. 4. Change of the rate of hydrogen production versus time in ethanol decomposition over Fe/Al_2O_3 catalysts with different loadings of Fe. (feeding rate of ethanol: 0.3 ml/h, carrier gas (Ar): 40 ml/min, reaction time: 3 h).

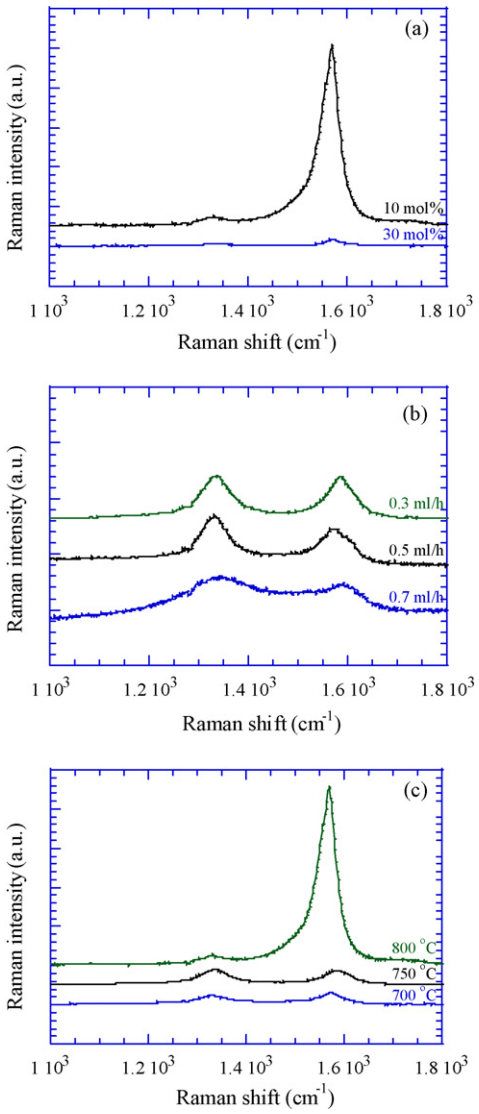

Fig. 5. Raman spectra of carbon deposited for: (a) different loadings of catalysts at 800 °C, feeding rate of ethanol: 0.3 ml/h; (b) 10 mol% loading of catalyst with different feeding rates of ethanol at 750 °C; (c) 10 mol% loading of catalyst at different reaction temperatures with fixed feeding rate (0.3 ml/h) of ethanol.

3.2. CNTs produced from ethanol decomposition

Multi-wall CNTs besides H_2 were also obtained from ethanol decomposition over Fe/Al_2O_3 catalysts. Raman spectroscopy, SEM, TEM and TG–DTG were used for characterization of CNTs produced under various experimental conditions (temperature, loading amount of Fe, and feeding rate of ethanol) to determine the optimal growth conditions for CNTs.

Raman spectra analysis is one of the significant methods to characterize CNTs. They include lots of information about the structure and properties of CNTs. There are two peaks at 1580 and 1354 cm^{-1} corresponding to G and D bands, respectively. The G band is associated with highly ordered graphite. The D band is related to amorphous carbon and the impurities and defects in CNTs. The ratio of the G to D band intensity (I_G/I_D) indicates the purity of CNTs, and the high I_G/I_D value conforms to high purity and less defects in sidewall of CNTs [24,25].

Fig. 5(a) shows Raman spectra of CNTs produced by ethanol decomposition over Fe/Al_2O_3 catalysts with Fe loadings of 10 and 30 mol% at 800 °C (the feeding rate of ethanol: 0.3 ml/h). CNTs formed for catalyst of 10 mol% loading had a very high G peak and very high I_G/I_D. This indicated that CNTs deposited over Fe/Al_2O_3 catalysts with 10 mol% loading had higher purity compared to other loadings under the same conditions. This result is also in agreement with that ethanol decomposition over the catalysts of 10 mol% Fe loadings could produce the highest yield of H_2 stated in Section 3.1.3.

Fig. 5(b) shows Raman spectra of CNTs deposited on 10 mol% loading of catalyst at the different feeding rates of ethanol (0.3, 0.5 and 0.7 ml/h) at 750 °C. As shown in Fig. 5, the feeding rate of ethanol had a little effect on I_G/I_D. However, CNTs formed at the lower feeding rate of ethanol (0.3 ml/h) had relatively higher I_G/I_D than that at the higher feeding rate.

Fig. 5(c) shows Raman spectra of CNTs deposited on Fe (10 mol%)/Al_2O_3 at different temperatures (the feeding rate of ethanol: 0.3 ml/h). We conclude from Fig. 5(c) that the temperature is a very important factor for producing CNTs with high quality. The I_G/I_D increased with reaction temperatures, being highest at 800 °C.

Fig. 6 shows SEM images of CNTs deposited by ethanol decomposition over Fe/Al_2O_3 catalysts with Fe loadings of 10, 20 and 30 mol% at 750 °C (the feeding rate of ethanol: 0.3 ml/h). From Fig. 6(a) a lot of branch-like CNTs with uniform diameter were observed on the particles of Fe (10 mol%)/Al_2O_3; but there were almost no CNTs formed on Fe (20 mol%)/Al_2O_3 besides amorphous carbon in Fig. 6(b). A few of CNTs with uneven diameter distribution deposited on Fe (30 mol%)/Al_2O_3 were presented in Fig. 6(c). With respect to no CNTs formed on Fe (20 mol%)/Al_2O_3, we cannot give a reasonable explanation for this strange result shown in Fig. 6(b).

Fig. 7 shows SEM images of CNTs deposited on 10 mol% Fe loading of catalyst with different feeding rates of ethanol at 750 °C. Fig. 7(a–c) correspond to 0.3, 0.5 and 0.7 ml/h (the feeding rate of ethanol) accordingly. CNTs produced at the lower feeding rate of ethanol (0.3 ml/h) had uniform diameter and high amounts. The amounts of CNTs decreased sharply with an increase of the feeding rate of ethanol, and there were almost no CNTs formed when the feeding rate of ethanol exceeded 0.7 ml/h.

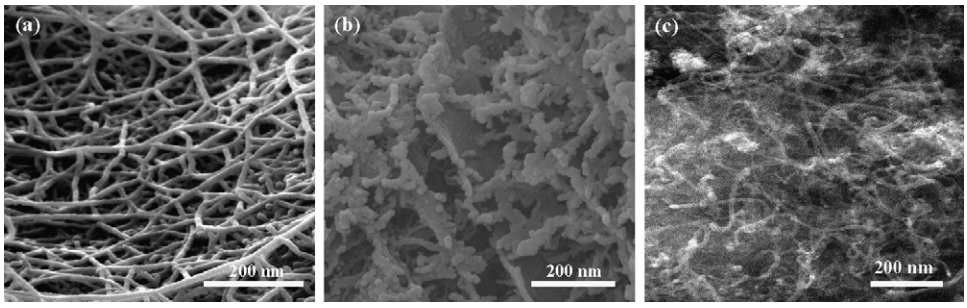

Fig. 6. SEM images of carbon deposited on the catalysts with different Fe loadings at 750 °C: (a) Fe (10 mol%)/Al_2O_3, (b) Fe (20 mol%)/Al_2O_3, (c) Fe (30 mol%)/Al_2O_3.

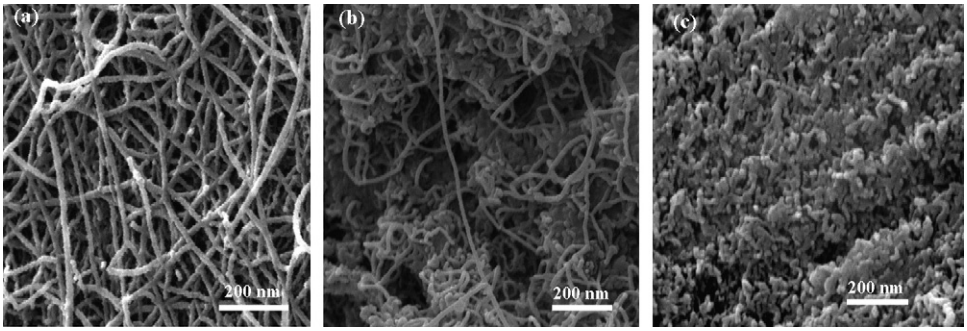

Fig. 7. SEM images of carbon deposited on catalysts at different feeding rates of ethanol for 10 mol% loadings of catalysts: (a) 0.3 ml/h; (b) 0.5 ml/h; (c) 0.7 ml/h.

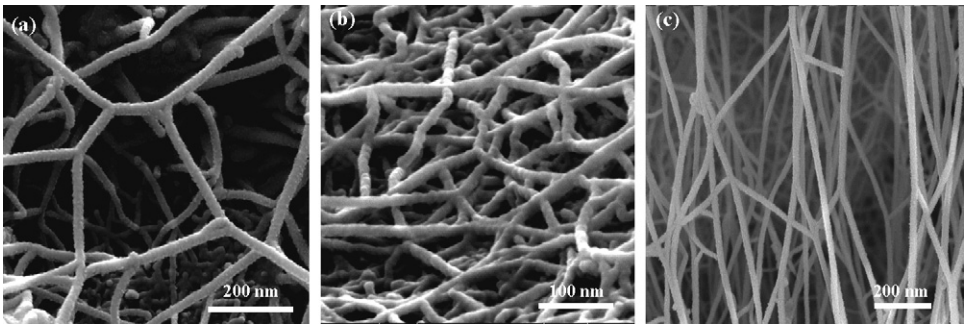

Fig. 8. SEM images of carbon deposited on catalysts at different temperatures for 10 mol% loadings of catalysts: (a) 700 °C; (b) 750 °C; (c) 800 °C.

Fig. 8 shows SEM images of CNTs deposited on 10 mol% loading of catalyst at different temperatures (the feeding rate of ethanol: 0.3 ml/h). The temperature was a very significant factor for producing high quality CNTs. There were web-like CNTs (Fig. 8(a)) formed at 700 °C; abundant branch-like CNTs (Fig. 8(b)) were produced at 750 °C, and with uniform distribution of diameter; when the temperature increased to 800 °C, CNTs with high quality, uniform diameter and well-oriented growth (Fig. 8(c)) were obtained.

Fig. 9 shows TEM images of as-grown CNTs on Fe (10 mol%)/Al_2O_3 at 800 °C with 0.3 ml/h feeding rate of ethanol. The multi-wall CNTs in Fig. 9 were with tube-walls of 2–3 layers and uniform diameters in the range of 8–10 nm.

TG–DTG analysis could be used to measure the yield of CNTs formed in the reaction [26,27]. TG–DTG curves of CNTs deposited on Fe (10 mol%)/Al_2O_3 at 800 °C (the feeding rate of ethanol: 0.3 ml/h) were measured with a heating rate of 10 °C/min in air and represented in Fig. 10. There are two obvious mass-loss steps for the sample tested in the temperature range of 25–1100 °C. This indicates that there are two kinds of carbon structure in reaction productions. According to the literature [26,27], the first mass-loss step generally arises from the loss of amorphous carbon and moisture. Amorphous carbon is easily oxidized in air at lower temperature (about 320 °C) and the first mass-loss is about 6%. The second mass-loss step results from CNTs. CNTs with regular graphite-structure are not easily oxidized until the temperature increases to about 750 °C and the second mass-loss is about 12%. That is to say, CNTs produced from ethanol decomposition is 12% of the total mass-containing amorphous carbon, CNTs and Fe/Al_2O_3 catalyst. Hereby, we can calculate the yield of CNTs under this kind of reaction conditions. The formula to calculate the yield of CNTs is as follows:

$$\text{CNTs yield}(\%) = \frac{m_{\text{CNT}}}{m_{\text{CAT}}} \times 100$$

where m_{CNT} is the mass of CNTs formed during ethanol decomposition and m_{CAT} is the mass of Fe contained in Fe/Al_2O_3 catalyst. It is calculated as the yield of CNTs formed on Fe

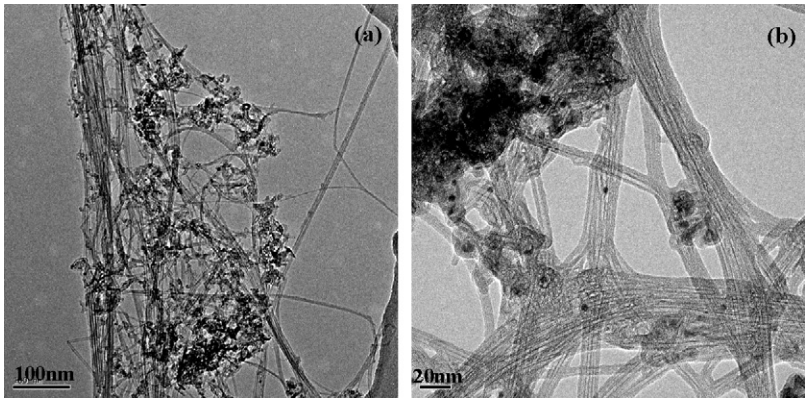

Fig. 9. TEM images of CNTs formed on Fe (10 mol%)/Al_2O_3 at 800 °C (feeding rate of ethanol: 0.3 ml/h).

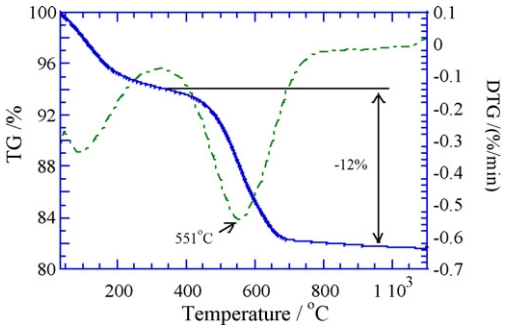

Fig. 10. TG–DTG curves of carbon deposited on Fe (10 mol%)/Al_2O_3 at 800 °C.

(10 mol%)/Al_2O_3 at 800 °C is 141% according to this formula and the results shown in Fig. 10.

3.3. The reactions of ethanol decomposition

The total tail gases produced from ethanol decomposition over Fe/Al_2O_3 catalysts in the reaction temperature ranges 500–800 °C was detected by on-line GC. It is found that three peaks at 0.5, 1.3 and 2.7 min, attributed to H_2, CO and CH_4, respectively, were observed from the chromatogram in the temperature range 500–700 °C, and the peak at 2.7 min gradually decreased with increasing temperature. When the temperature reached 800 °C, no peak corresponded to CH_4 was found (detection limit of CH_4, 20 ppm), only H_2 and CO products were detected. This phenomenon indicated that CH_4 contained in tail gases was further decomposed into carbon and H_2 when temperature increased and even disappeared at temperature 800 or higher than 800 °C. Based on the results above, the following equations probably better describe the processes of ethanol decomposition at different temperatures:

$$CH_3CH_2OH \rightarrow CO + H_2 + CH_4, \Delta H^\circ = 49.76\,kJ\,mol^{-1} \quad (1)$$

$$CH_4 \rightarrow C + 2H_2, \Delta H^\circ = 74.81\,kJ\,mol^{-1} \quad (2)$$

$$CH_3CH_2OH \rightarrow C + CO + 3H_2, \Delta H^\circ = 124.58\,kJ\,mol^{-1} \quad (3)$$

It can be found that reaction 1 plus 2 is reaction 3, and all of them are heat-absorbing reaction. Their reaction enthalpies (ΔH°) increase in the order of reaction 1 < reaction 2 < reaction 3. From the viewpoint of thermodynamics, reaction 3 is more thermodynamically favored than reactions 1 and 2 at high temperature: H_2, CO and CH_4 could be detected and carbon deposition could be also observed on Fe/Al_2O_3 catalysts, whatever the loadings of catalysts, showing the occurrence of reaction 1 and subsequently partial reaction 2 at relatively lower temperature 500–700 °C. However, when the temperature increased to 800 °C reaction 2 could occur completely, i.e., reaction 3 started to take place. This is just the reason that no CH_4 was detected from the tail gases and the maximum ratio of hydrogen production higher than 80% could be achieved (Fig. 3).

4. Conclusions

In the present work, we studied systemically the ethanol decomposition for the co-production of H_2 and CNTs under different reaction conditions (temperature and feeding rate of ethanol). Fe/Al_2O_3 catalysts have an obviously catalytic effect in the co-production of H_2 and CNTs from ethanol decomposition, and the activity and stability of Fe/Al_2O_3 catalysts depend strongly on the loading amount of Fe. Carbon deposited on Fe (10 mol%)/Al_2O_3 catalyst at 800 °C (the feeding rate of ethanol: 0.3 ml/h) was multi-wall CNTs and presented the best quality. The yield of CNTs synthesized was 141%. Considering the ratio of hydrogen production, the total H_2 yield and the quality of formed CNTs, the Fe (10 mol%)/Al_2O_3 catalyst was the best one for the co-production of H_2 and CNTs from ethanol decomposition. In addition, the reaction of ethanol decomposition was proposed.

Acknowledgements

The authors acknowledge the financial supports of the National Hi-Tech Research and Development Program (863) of China (No. 2007AA05Z116), the financial supports of the National Natural Science Foundation of China (No.20673082), the scientific research foundation for ROCS, SEM. (No.2006331), the key project of science and technology of Shaanxi Province (No.2005k07-G2), the natural science foundation of Shaanxi education Committee (No.06JK167), and the NWU Graduate Cross-discipline Funds (No.07YJC03). The authors are also grateful to the State Key Laboratory of Continental Dynamics for the SEM measurements.

References

[1] H. Wang, S. Takenaka, K. Otsuka, Int. J. Hydrogen Energy 31 (2006) 1732.
[2] T.N. Veziroglu, F. Barbir, Int. J. Hydrogen Energy 17 (1992) 391.
[3] P. Kruger, Int. J. Hydrogen Energy 25 (2000) 1023.
[4] P. Kruger, Int. J. Hydrogen Energy 26 (2001) 1137.
[5] P.Y. Sheng, A. Yee, G.A. Bowmaker, H. Idriss, J. Catal. 208 (2002) 393.
[6] A. Haryanto, S. Fernando, N. Murali, S. Adhikari, Energy Fuels 19 (2005) 2098.
[7] T. Davidian, N. Guilhaume, E. Iojoiu, H. Provendier, C. Mirodatos, Appl. Catal. B: Environ. 73 (2007) 116.
[8] K. Faungnawakij, Y. Tanaka, N. Shimoda, T. Fukunaga, R. Kikuchi, K. Eguchi, Appl. Catal. B: Environ. 74 (2007) 144.
[9] S. Takenaka, Y. Shigeta, E. Tanabe, K. Otsuka, J. Catal. 220 (2003) 468.
[10] H. Ogihara, S. Takenaka, I. Yamanaka, E. Tanabe, A. Genseki, K. Otsuka, J. Catal. 238 (2006) 353.
[11] M.A. Goula, S.K. Kontou, P.E. Tsiakaras, Appl. Catal. B 49 (2004) 135.
[12] S.R. Segal, K.A. Carrado, C.L. Marshall, K.B. Anderson, Appl. Catal. A 248 (2003) 33.
[13] D.K. Liguras, D.I. Kondarides, X.E. Verykios, Appl. Catal. B 43 (2003) 345.
[14] N. Laosiripojana, S. Assabumrungrat, Appl. Catal. B: Environ. 66 (2006) 29.
[15] Y.Z. Yang, C.-H. Chang, H. Idriss, Appl. Catal. B: Environ. 67 (2006) 217.
[16] S. Iijima, Nature 354 (1991) 56.
[17] V.N. Popov, Mater. Sci. Eng. R 43 (2004) 61.
[18] R.H. Baughman, A.A. Zakhidov, W.A. de Heer, Science 297 (2002) 787.
[19] T.W. Ebbesen, P.M. Ajayan, Nature 358 (1992) 220.
[20] T. Guo, P. Nikolaev, A. Thess, D.T. Colbert, R.E. Smalley, Chem. Phys. Lett. 243 (1995) 49.
[21] J.F. Colomer, C. Stephan, S. Lefrant, G. Van Tendeloo, I. Willems, Z. Konya, A. Fonseca, Ch. Laurent, J.B. Nagy, Chem. Phys. Lett. 317 (2000) 83.
[22] M. Pérez-Cabero, I. Rodríguez-Ramos, A. Guerrero-Ruíz, J. Catal. 215 (2003) 305.
[23] S. Maruyama, R. Kojima, Y. Miyauchi, S. Chiashi, M. Kohno, Chem. Phys. Lett. 360 (2002) 229.
[24] A.M. Rao, E. Richter, S. Bandow, B. Chase, P.C. Eklund, K.A. Williams, S. Fang, K.R. Subbaswamy, M. Menon, A. Thess, R.E. Smalley, G. Dresselhaus, M.S. Dresselhaus, Science 275 (1997) 187.
[25] M.R. Maschmann, P.B. Amama, A. Goyal, Z. Iqbal, R. Gat, T.S. Fisher, Carbon 44 (2006) 10.
[26] C.H. Li, K.F. Yao, J. Liang, Appl. Catal. A 261 (2004) 221.
[27] Z.J. Shi, Y.F. Lian, F.H. Liao, X.H. Zhou, Z.N. Gu, Y. Zhang, S. Iijima, H.D. Li, K.T. Yue, S.L. Zhang, J. Phys. Chem. Solids 61 (2000) 1031.